



# Absolute myocardial blood flows derived by dynamic CZT scan vs invasive fractional flow reserve: Correlation and accuracy

Konstantin V. Zavadovsky, MD,<sup>a</sup> Andrew V. Mochula, PhD,<sup>a</sup>  
Alla A. Boshchenko, MD,<sup>a</sup> Alexander V. Vrublevsky, MD,<sup>a</sup> Andrew E. Baev,  
PhD,<sup>a</sup> Alexander L. Krylov, MD,<sup>a</sup> Marina O. Gulya, PhD,<sup>a</sup>  
Evgeny A. Nesterov, PhD,<sup>b</sup> Riccardo Liga, MD,<sup>c</sup> and Alessia Gimelli, MD<sup>d</sup>

<sup>a</sup> Cardiology Research Institute, Tomsk National Research Medical Centre, Russian Academy of Sciences, Tomsk, Russia

<sup>b</sup> National Research Tomsk Polytechnic University, Tomsk, Russia

<sup>c</sup> Università di Pisa, Pisa, Italy

<sup>d</sup> Fondazione Toscana/CNR Gabriele Monasterio, Pisa, Italy

Received Nov 2, 2018; accepted Feb 21, 2019

doi:10.1007/s12350-019-01678-z

**Purpose.** To define the diagnostic power of absolute myocardial blood flow (MBF) evaluation on dynamic CZT imaging in intermediate risk patients in comparison with invasive coronary angiography (ICA) and fractional flow reserve (FFR).

**Methods.** Twenty-three stable CAD patients underwent one-day dynamic rest-stress <sup>99m</sup>Tc-Sestamibi myocardial perfusion imaging by CZT camera. Stress and rest MBF values were calculated semi-automatically using a net retention model by Leppo. Coronary flow reserve (CFR) and flow difference (FD) [MBF stress – MBF rest] were also estimated. A total of 28 vessels were functionally quantified with FFR: 19 (68%) vessels with a stenosis ≥ 70% and 9 (32%) with < 70% stenotic lesions.

**Results.** The mean global MBFs at rest and during stress were 0.36 (IQR 0.33-0.54) mL/min/g and 0.67 (IQR 0.55-0.81) mL/min/g, respectively, with an average CFR of 1.80 (IQR 1.35-2.24). Moderate correlations between stenosis severity and FFR ( $r = 0.45$ ;  $P = .01$ ), stress MBF ( $r = -0.46$ ;  $P = .01$ ) and FD ( $r = -0.37$ ;  $P = .04$ ) were detected. FFR abnormalities were best predicted by absolute stress MBF, CFR and FD with values of ≤ 0.54 mL/min/g (sensitivity 61.5%; specificity 93.3%), ≤ 1.48 (sensitivity 69.2%; specificity 93.3%) and ≤ 0.18 mL/min/g (sensitivity 69.2%; specificity 100%), respectively.

**Conclusions.** The values of stress MBF, CFR and FD obtained through dynamic CZT acquisitions compare well with invasive FFR. The clinical use of dynamic acquisition of myocardial perfusion imaging by CZT may help cardiologist in the detection of hemodynamically significant CAD. (J Nucl Cardiol 2021;28:249–59.)

**Electronic supplementary material** The online version of this article (<https://doi.org/10.1007/s12350-019-01678-z>) contains supplementary material, which is available to authorized users.

The authors of this article have provided a PowerPoint file, available for download at SpringerLink, which summarises the contents of the paper and is free for re-use at meetings and presentations. Search for the article DOI on SpringerLink.com

**Funding** Contribution of Evgeniy A. Nesterov from Tomsk Polytechnic University was funded by Tomsk Polytechnic University Competitiveness Enhancement Program Grant (VIU-Laboratory No. 31 YAR-221/2018).

All editorial decisions for this article, including selection of reviewers and the final decision, were made by guest editor Saurabh Malhotra, MD, MPH.

Reprint requests: Konstantin V. Zavadovsky, MD, Cardiology Research Institute, Tomsk National Research Medical Centre, Russian Academy of Sciences, Kievskaya Str 111A, Tomsk, Russia, 634012; [konstzav@gmail.com](mailto:konstzav@gmail.com)  
1071-3581/\$34.00

Copyright © 2019 American Society of Nuclear Cardiology.

**Key Words: Absolute myocardial blood flow • coronary flow reserve • CZT camera • fractional flow reserve**

**Abbreviations**

CAD	Coronary artery disease
CFR	Coronary flow reserve
CZT	Cadmium-zinc-telluride
FD	Flow difference
FFR	Fractional flow reserve
ICA	Invasive coronary angiography
MBF	Myocardial blood flow
MPI	Myocardial perfusion imaging
SPECT	Single-photon emission computerized

**See related editorial, pp. 260–262**

**INTRODUCTION**

The adequate accuracy of traditional SPECT imaging in detecting coronary artery disease (CAD) has been already reported in different clinical settings; however, there are a number of conditions in which it may fail to detect the presence of functionally significant coronary stenosis, possibly missing the individuation of patients at risk of cardiac events. This aspect is related to the fact that traditional SPECT imaging offers only a semi-quantitative evaluation of regional myocardial perfusion, unable to assess subtle and/or diffuse alterations of myocardial blood flow (MBF) regulation that might solely be apparent with the quantification of absolute myocardial perfusion parameters.

While cardiac position emission tomography (PET) imaging would allow readily the quantification of MBF in absolute terms, the technical complexity and elevated operative costs of this methodology have prevented its application in the clinical arena.<sup>1–3</sup> In this respect, recent advancements in SPECT technology, particularly related to the introduction of dedicated cardiac cameras equipped with Cadmium-Zinc-Telluride (CZT) detectors, might possibly overcome most of the limitation of traditional SPECT systems.<sup>4–6</sup> As a matter of fact, the increasing of sensitivity, and opportunity to acquire dynamic tomographic data without rotation of detectors allows the quantitation of absolute MBF datasets.<sup>5</sup> In a very recent study conducted in high-cardiac risk population with known significant CAD, it was demonstrated that the evaluation of MBF with a dynamic CZT acquisition was technically feasible and provided similar values of coronary flow reserve (CFR) as compared to PET.<sup>6,7</sup> However, despite these initial results, no information is yet available on the accuracy and possible clinical value of MBF quantification by CZT in an

unselected population of suspected or known CAD patients.

Accordingly, we aimed at defining the diagnostic power of MBF evaluation on dynamic CZT imaging in a broad range of patients submitted to invasive coronary angiography (ICA) and fractional flow reserve (FFR).

**METHODS**

**Study Population**

The study group comprised 23 consecutive patients (12 women, 11 men, mean age  $61.2 \pm 6.8$  years) with stable chest pain and suspected ( $n = 11$ ) or known CAD ( $n = 12$ ). All patients underwent non-invasive assessment of MBF by dynamic <sup>99m</sup>Tc-Sestamibi CZT followed by ICA with FFR in the case of intermediate coronary lesions ( $\geq 30 < 70\%$  stenosis) within 7 days (average  $3.7 \pm 1.2$  days) from MPI. The exclusion criteria were: acute coronary syndrome, hemodynamic instability, myocardial inflammatory diseases, storage diseases, moderate-to-severe cardiac valvular disease, atrial fibrillation, contraindication to adenosine or iodine administration. Physicians performing ICA and CZT studies, respectively, were blinded to the results of the other technique.

Written informed consent was obtained from all patients and the study Protocol was approved by Local ethics Committee.

**Standard and Dynamic Myocardial Perfusion Imaging**

All patients underwent a one-day rest-stress dynamic and conventional acquisition on CZT camera (GE Discovery NM/CT 570C). Myocardial perfusion imaging (MPI) scans were acquired using low-energy multi-pinhole collimator and 19 stationary detectors simultaneously imaging 19 different views without detector rotation. Each detector contained  $32 \times 32$  pixelated ( $2.46 \times 2.46$  mm) CZT elements 20% energy window at 140 keV was used.

**Patient preparation** Patients were instructed to refrain from caffeine and methylxanthine-containing substances and to avoid nitrates, calcium channel blockers and beta-blockers for at least 24 hours before the scan. All scans were performed after an overnight fasting.

**Patient positioning** All patients were imaged in the supine position with arms placed over their heads. Before the first dynamic acquisition, a low-dose CT scan was performed to correct positioning the heart in the gamma-camera centre of the field of view. The same data were used for attenuation correction. Tube voltage was setting on 120 kV, tube current on 20 mA, rotation time on 0.8 seconds, helical pitch 0.969:1, slice thickness on 5 mm, and interstice interval on 5 mm.

**Dynamic SPECT data acquisition** A rest-stress single-day protocol was performed in all patients. A dose of 3 MBq/kg of <sup>99m</sup>Tc Sestamibi was injected at rest using a shielded syringe pump intravenously as a 3 mL bolus (injection rate 1 mL/s) followed by saline flush (5 mL with the rate 1 mL/s). List mode ECG-gated dynamic data acquisition started just prior to the radiopharmaceutical bolus injection and acquired for 360 seconds. Then, the patients were removed from the scanner. After 45 minutes from rest tracer injection, a standard CZT rest acquisition were performed, using a dedicated patient positioning tool to obtain the same coordinates of the heart as in the previous scan. The standard CZT rest scan was acquired for 7 minutes. At the end of rest acquisition, all patients were submitted to stress test and dynamic acquisition, without moving from the camera.

After 2 minutes of intravenous infusion of adenosine (140 mcg/kg/min), a second dose of <sup>99m</sup>Tc Sestamibi (9 MBq/kg) was injected and list mode dynamic data acquisition of 360 seconds was started just prior to the injection. The infusion of adenosine continued for 2 minutes more, accordingly to standard protocol.<sup>8</sup> After that, as for rest scan, the patients were removed from the gamma-camera and a stress standard scan was acquired after 45 minutes after the tracer injection.

The mean <sup>99m</sup>Tc-MIBI dose at rest was  $245.3 \pm 42.3$  MBq (range 192–360 MBq); at stress  $736.0 \pm 127.0$  (range 576–1080 MBq). The mean effective radiation dose was  $8.02 \pm 1.38$  mSv per patient. The entire acquisition protocol takes 125 min. Before, throughout, and after the infusion of vasodilator, heart rate, systemic blood pressure, and 12-lead electrocardiogram (ECG) were monitored. No major side-effects were documented during the stress test in the whole population.

## ICA and FFR Assessment

All patients underwent quantitative coronary arteriography on an Axiom Artis coronary angiography system (Siemens; Erlangen, Germany). FFR assessment was performed using ILUMIEN console (St. Jude Medical, St. Paul, MN, USA) and 0.014" pressure-monitoring Wire Aeris (St. Jude Medical). After intracoronary administration of 100 mcg nitroglycerine, baseline pressure was measured in the ostium of the target coronary artery and distal to the particular lesion. To induce maximal coronary blood flow intravenous infusion of adenosine (140 mcg per kilogram per minute) was used. FFR was calculated as a ratio of the mean intracoronary pressure (0.5–2.0 cm distal to the lesion) to the mean pressure in the ostium of the coronary artery during the steady-state (60–90 seconds) hyperemia. Significant CAD was considered by invasive coronary angiography as > 50% stenosis of the left main stem, > 70% stenosis in a major coronary vessel.<sup>9</sup> The FFR values  $\leq 0.80$  were deemed indicative of significant inducible ischemia.

## Data Analysis

**Conventional CZT data reconstruction** Low-dose CT scans were transferred to Xeleris workstation to obtain attenuation maps for attenuation

correction. CZT images were reconstructed on the dedicated workstation (Xeleris 4.0; GE Healthcare, Haifa, Israel) using maximum-penalized-likelihood iterative reconstruction (60 iterations; Green OSL Alpha 0.7; Green OSL Beta 0.3) to acquire perfusion images in standard cardiac axes (short axis, vertical long axis, and horizontal long axis). The software Myovation for Alcyone (GE Healthcare, Haifa, Israel) was used for image reconstruction, and Butterworth post-processing filter (frequency 0.37; order 7) was applied to the reconstructed slices. The reconstruction was performed in  $70 \times 70$  pixels matrix with 50 slices.

Raw MPI-CZT data at stress and at rest were visually analysed for motion and attenuation artefacts. Stress/rest images were analysed with a commercially available software package Corridor 4DM (University of Michigan, Ann Arbor, MI, USA). The calculation of MPI parameters was performed based on uncorrected and attenuation corrected image analysis.

Each of 17 segments was scored based on semiquantitative 5-point scoring system (from 0 = normal uptake to 4 = absent radiotracer distribution).<sup>10</sup> Accordingly, the sum of the stress scores of all segments (SSS) and the sum of the rest scores of all segments (SRS) were quantified. A summed difference score (SDS) was calculated as the difference between SSS and SRS. A fixed perfusion defect was identified when SSS and SRS > 4 combined with SDS < 2; a reversible perfusion defect when SSS was  $\geq 4$ , SRS < 4 with SDS  $\geq 2$ . A per-patient and per-vessel analysis was performed.

## Dynamic CZT Data Analysis

Each rest-stress list-file acquisition data were evaluated using a dedicated software (Corridor 4DM for Alcyone, v2015, INVIA, Ann Arbor, MI, USA). The acquired data were initially reconstructed (in  $70 \times 70$  pixels matrix; 50 slices) and re-binned with "CFR reframe" into 44 frames: 40 frames of 4.5 seconds each and 4 frames of 45 seconds each. Using CFR CrossTalk application, dynamic images of rest residual activity at the time of stress injection were created by down-scaling the perfusion data according to tracer decay and CZT acquisition duration. The reframed and corrected (for stress dataset) dynamic images were reconstructed using penalized maximum likelihood expectation maximization iterative algorithm (60 iterations; regularization type: OSL green; Green OSL Alpha 0.7, Green OSL Beta 0.5). Finally, the reconstructed dynamic images as well as CT attenuation correction maps were processed by 4DM Reserve application. No major motion and/or attenuation artefacts were present on the raw MPI-CZT data.

The appropriateness of LV contours and blood flow sampling ROI location were checked and adjusted (if necessary) manually. The time-activity curves (TAC) for the input function and whole left ventricular myocardium as well as for the LAD, LCx and RCA vessel territories were generated semi-automatically. The ROI for input function was located on the valve plane and including parts of LV cavity and left atrium. The size of this ROI was 4 mm on short-axis view and 30 mm on long-axis views.

The myocardial retention rate was estimated using generalized net retention model<sup>11,12</sup> with standard settings:

$$R = \frac{\frac{1}{PV} \times \frac{1}{(t_3 - t_2)} \int_{t_2}^{t_3} C_m(t) dt - S_m \times C_a(t) dt}{CF \int_0^{t_1} C_a(t) dt - S_b \times C_m(t) dt}$$

In this equation, *R* is the retention rate; *PV* is the partial volume correction value, was set to 0.84; *C<sub>m</sub> (t)* is the measured myocardial tissue TAC; *C<sub>a</sub> (t)* is the measured input function TAC; *CF* is the correction factor, was set to 1.00; *S<sub>m</sub>* is the spillover from the blood pool into the myocardium, was set to 0.40<sup>13,14</sup>; *S<sub>b</sub>* is the spillover from the myocardium into the blood pool, was set to 0.0<sup>15</sup>; the time limit *t<sub>1</sub>* is the upper limit of integration of blood pool curve, *t<sub>2</sub>* is the lower limit of integration of the tissue curve, and *t<sub>3</sub>* is the upper limit of integration of the tissue curve. The values for *t<sub>1</sub>*, *t<sub>2</sub>*, and *t<sub>3</sub>* were set to 60, 60 and 120 seconds respectively.

To convert the tracer retention ratio to MBF values the Renkin–Crone flow model was used using parameters  $\alpha = 0.874$ ,  $\beta = 0.443$ <sup>11</sup>:

$$R = MBF \times (1 - \alpha \times e^{-\frac{\beta}{MBF}})$$

The value of CFR was calculated as MBF ratio (MBF stress/MBF rest). Additionally, the absolute difference between stress MBF and rest MBF as flow difference (FD) was calculated.<sup>2,16</sup> To identify relationships between dynamic CZT and invasive FFR, the values of FFR measurement in the specific artery and the corresponding regional stress MBR, CFR and FD values were used.

### Statistical Analysis

The distribution of continuous variables was checked using the Shapiro-Wilk *W*-test. Continuous variables were expressed as mean ± standard deviation and as median with quartiles (Q<sub>25</sub> to Q<sub>75</sub>). Spearman test was used to estimate the correlation coefficient between quantitative variables. The receiver-operating-characteristic (ROC) curve analysis was performed to evaluate the sensitivity and specificity of MPI indices to predict FFR ≥ 0.8. The values of areas under curve (AUC) were compared by the DeLong method.<sup>17</sup> Values were considered statistically significant when *P* was < .05. Statistical analyses were performed using SPSS statistical software 19.0 (SPSS Inc., Chicago, IL, USA) and Medcalc version 17.4 (MedCalc Software, Mariakerke, Belgium).

## RESULTS

The demographic and clinical characteristics of the patients enrolled, including cardiovascular risk factors and drug therapies, are reported in Table 1. Of notice, 8 (35%) patients had typical angina, 15 (65%) patients had atypical chest pain.

### MPI Results

Rest/stress CZT imaging was completed in all patients without adverse events. Ten (43%) patients presented a homogeneous myocardial perfusion both at rest and during stress, while 13 (57%) had evidence of

inducible myocardial ischemia, involving the LAD, LCX, and RCA coronary territory in 7, 3, and 6 patients, respectively. On dynamic CZT evaluation, the mean global MBFs at rest were 0.36 (range 0.33-0.54) mL/min/g, and during stress were 0.67 (range 0.55-0.81) mL/min/g, respectively, with an average CFR of 1.80 (range 1.35-2.24) (Table 2). The analysis of semi-quantitative and quantitative myocardial perfusion parameters identified a correlation among SDS and global CFR (*r* = − 0.45; *P* = .03) as well as among SDS and global FD (*r* = − 0.42; *P* = .04).

### ICA Results

According to the patient-based analysis, significant CAD was present in 16 (70%) patients. This cohort included seven (30%) patients with one-vessel, seven (30%) with two-vessel and two (9%) with triple-vessel disease. Among them, complete coronary occlusions were revealed in two patients. Seven (30%) patients had non-obstructive CAD. The per-vessel analysis identified 67 stenotic lesions: 21/67 with a stenosis > 70% (8/21 on LAD, 8/21 on LCx and 5/21 on RCA), 46/67 with a stenosis > 50% and ≤ 70% (18/46 on LAD, 9/46 on LCx and 13/46 on RCA) and 6 stenosis < 50% on LM.

Coronary artery stenoses were located in proximal, middle and distal coronary artery segments in 42 (63%), 14 (21%) and 11(16%) cases. A total 28 stenoses were functionally quantified with FFR: 2/28 in LM, 19/28 in LAD, 4/28 in LCx and 3/28 in RCA. FFR revealed significant ischemia in 8/19 stenoses 30-70%, in 6/9 > 70%.

Measurement of FFR was performed in all the stenotic vessels, with the exception of: presence of serial coronary artery stenosis (*n* = 6); small diameter vessels (*n* = 17); presence of stenosis < 30% (*n* = 2); coronary artery occlusion (*n* = 2); presence of stenosis > 70% with difficult/risky FFR assessment (i.e. angulation, tortuosity, severe calcification).

The average FFR value was 0.81 ± 0.4. A moderate correlation between stenosis severity and FFR values was revealed (*r* = − 0.45; *P* = .01). A weak correlations between stenosis severity and stress MBF (*r* = − 0.34; *P* = .003) as well as FD (*r* = − 0.28; *P* = .01) were detected. Interestingly, among the 10 patients with homogeneous myocardial perfusion on semiquantitative analysis, 6/10 presented CAD, with a multivessel involvement in three of them. In these patients with CAD, the global stress MBF values was significantly lower than in those without CAD: 0.64 mL/min/g (range 0.58-0.68 mL/min/g) vs 0.79 mL/min/g (range 0.76-1.17 mL/min/g) (*P* = .04), respectively.

**Table 1.** Clinical characteristics of the enrolled patients

BMI, kg/m <sup>2</sup>	28.5 ± 4.4
Systolic BP (mmHg)	144 ± 24.8
Diastolic BP (mmHg)	84.7 ± 9.3
HR (beats/min)	67.8 ± 12.0
Hypercholesterolemia, including	17 (74%)
Achieved target level	10 (59%)
Not achieved target level	7 (41%)
Hypertension	20 (87%)
Diabetes mellitus (type 2)	5 (22%)
Typical angina	8 (35%)
Atypical angina	15 (65%)
NYHA:	
Class I	18 (78%)
Class II	1 (4%)
Extra-systoles	6 (26%)
Any carotid atherosclerosis	17 (74%)
Any peripheral atherosclerosis	15 (65%)
Prior myocardial infarction (Q-, non-Q)	11 (47%)
EF (%)	64.2 ± 6.4
EFLV > 50%, n (%)	22 (96%)
EFLV 40–0%, n (%)	1 (4%)
EDV (mL)	97.4 ± 24.8
ESV (mL)	37.8 ± 13.3
Pharmacological treatment	
Beta-blockers	17 (74%)
Calcium channel blockers	6 (26%)
Nitrates	4 (17%)
ACE inhibitors	14 (61%)
Antagonists of AT-receptors	7 (30%)
Aspirin	23 (100%)
Other antiplatelet drugs	16 (70%)
Statins	23 (100%)
Other	4 (17%)

### Combined Anatomic-Functional Analysis: Per-vessel Analysis

The interaction between coronary stenosis severity and regional MPI perfusion parameters (SSS, SDS, stress MBF, CRF and FD) is illustrated in Figure 1. Regional MBF, CFR and FD showed significant correlations with FFR values: rMBF ( $r = 0.63$ ;  $P < .001$ ), rCFR ( $r = 0.66$ ;  $P < .01$ ) and rFD ( $r = 0.73$ ;  $P < .01$ ), (Figure 2). Accordingly, on ROC analysis, abnormal FFR values were best predicted by CZT-derived absolute stress MBF, CFR and FD with values of  $\leq 0.54$  mL/min/g (sensitivity 61.5%; specificity 93.3%),  $\leq 1.48$  (sensitivity 69.2%; specificity 93.3%) and  $\leq 0.18$  mL/min/g (sensitivity 69.2%; specificity 100%), respectively

**Table 2.** The values of global and regional myocardial blood flow and coronary flow reserve (median and interquartile range)

Index	Value
Rest LAD MBF (mL/min/g)	0.37 (0.27; 0.62)
Rest LCX MBF (mL/min/g)	0.40 (0.28; 0.67)
Rest RCA MBF (mL/min/g)	0.36 (0.31; 0.52)
Rest global MBF (mL/min/g)	0.36 (0.33; 0.54)
Stress LAD MBF (mL/min/g)	0.62 (0.42; 0.91) <sup>a</sup>
Stress LCX MBF (mL/min/g)	0.84 (0.5; 0.98) <sup>a</sup>
Stress RCA MBF (mL/min/g)	0.63 (0.48; 0.91) <sup>a</sup>
Stress global MBF (mL/min/g)	0.67 (0.55; 0.81) <sup>a</sup>
LAD CFR (S/R)	1.81 (1.35; 2.09)
LCx CFR (S/R)	1.87 (1.42; 2.54)
RCA CFR (S/R)	1.81 (1.08; 2.22)
Global CFR (S/R)	1.80 (1.35; 2.24)
LAD FD (mL/min/g)	0.27 (0.12; 0.40)
LCX FD (mL/min/g)	0.37 (0.15; 0.70)
RCA FD (mL/min/g)	0.34 (0.04; 0.51)
Global FD (mL/min/g)	0.27 (0.14; 0.47)

LAD, left anterior descending artery; LCX, left circumflex artery; RCA, right coronary artery; MBF, myocardial blood flow; CFR, coronary flow reserve; FD, flow difference  
<sup>a</sup>Wilcoxon test  $P$  value  $< .001$  (in comparison with rest values)

showing the highest accuracy in predicting the presence of invasively determined myocardial inducible ischemia (Figure 3). Specifically, when regional CFR was below the cut-off value of  $\leq 1.48$ , FFR was pathological in the 90% of the cases. Conversely, in the case of normal CFR values, FFR was preserved in the 78% of the cases.

Representative images of CFR measurement is shown in Figure 4.

## DISCUSSION

The present results indicate that the quantification of regional absolute myocardial perfusion parameters on dynamic CZT images is feasible in a real-life population of patients, comparing well with results obtained with the invasive gold-standard represented by FFR. Accordingly, quantitation of MBF and CFR on CZT allowed the identification of functionally significant CAD in the greatest majority of the case.

### Quantification of MBF on SPECT Imaging: Possible Clinical Applications

Current guidelines for the evaluation of patients with suspected or known CAD make the assessment of

the presence and extent of myocardial ischemia as a mandatory step in the global diagnostic process.<sup>18,19</sup> However, the reliability of myocardial ischemia evaluation depends on the specific non-invasive stress test that is adopted, each of whom is characterized by a different accuracy in detecting CAD, performing differently in specific clinical settings (i.e., perfusion vs wall motion analysis).<sup>20</sup> In this context, MPI on SPECT is among the most performed imaging stress tests for the evaluation of myocardial ischemia,<sup>21</sup> it may sometimes show a sub-optimal accuracy in identifying patients with significant CAD.<sup>22</sup> In patients with a diffusely reduced MBF, traditional SPECT imaging may fail to identify regional differences of myocardial perfusion, possibly missing patients at risk of future cardiac events. Interestingly, this condition may develop in disparate clinical settings, such as triple-vessel CAD,<sup>23–25</sup> diffuse non-significant atherosclerosis,<sup>26</sup> and/or microvascular dysfunction,<sup>27</sup> conditions in which the absolute evaluation of MBF might offer clear advantages in the characterization of the underlying myocardial ischemic burden.<sup>16</sup> While some attempts have been performed,<sup>28–30</sup> the recent introduction of high-efficiency dedicated SPECT cameras equipped with CZT detectors has given new interest on this area of investigation, with some recent reports suggesting the relative feasibility of MBF evaluation in highly selected populations of patients.<sup>5,7,31,32</sup> Our

results seem to indicate that the flow ranges obtained with dynamic CZT imaging are relatively lower than the ones classically reported with PET. However, differences in terms of tracer’s kinetics between the two methodologies likely explain most of the variability. As a matter of fact, as previously demonstrated, the <sup>99m</sup>Tc-labeled tracer’s retention is lower in comparison with PET tracers, particularly at high flow rates.<sup>11</sup> Moreover, the spatial resolution of SPECT is lower than that of PET, further influencing the comparison between the two techniques. Nevertheless, the MBF values obtained with our analysis were able to predict FFR abnormalities with an elevated specificity, being generally in the range of the MBFs obtained by other groups using the same camera.<sup>7</sup> Finally, the one-tissue-compartment model analysis, used in the study published by Nkolou R. and colleagues, for the evaluation of MBF, and net-retention model are based on different algorithms and this could explain the difference in terms of given results.<sup>11,12,33</sup> Additional studies are needed to estimate suitable correction coefficients to convert retention to MBF using one-tissue compartment as well as net retention models with <sup>99m</sup>Tc-labeled tracers. The clinical impact of relatively low values of MBF in our study could be reduced by taking the ratio of stress and rest flow to produce a measure of CFR.

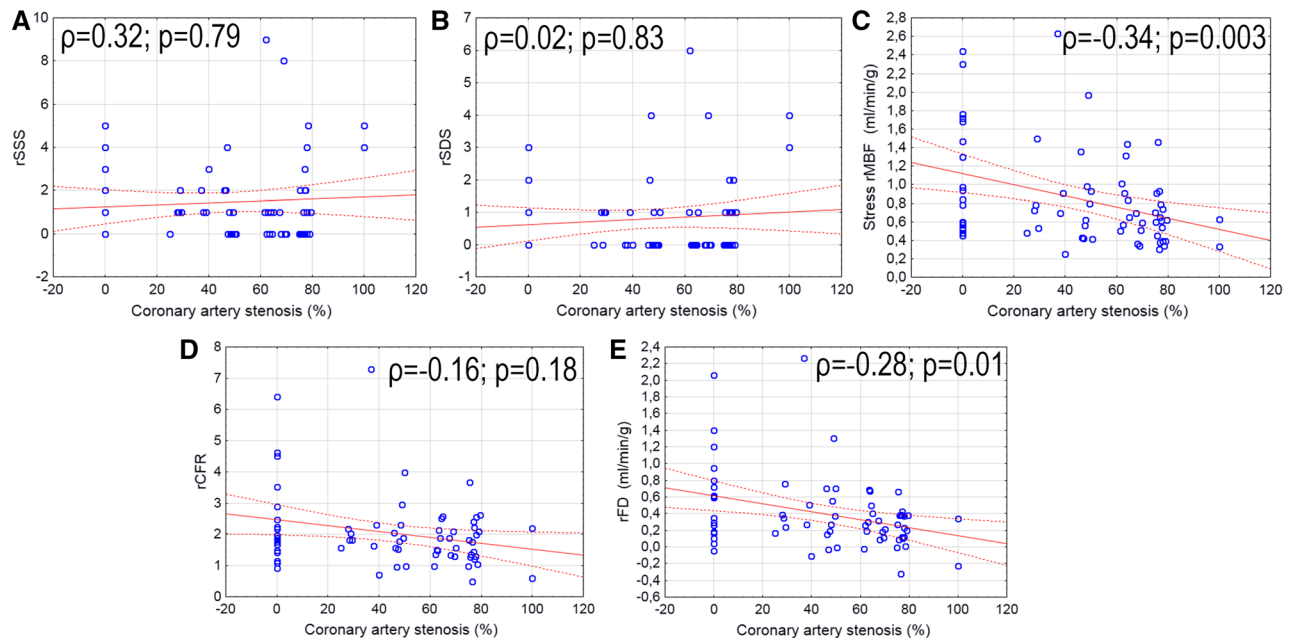


**Figure 1.** Correlations between coronary artery stenosis severity and corresponding regional MPI parameters: (A) rSSS; (B) rSDS; (C) stress rMBF; (D) rCFR; (E) rFD. The solid line corresponds to the best-fit line and the dashed lines indicate the 95% mean confidence interval. rSSS, regional summed stress score; rSDS, regional summed difference score; stress rMBF, regional myocardial blood flow; rCFR, regional coronary flow reserve; rFD, regional flow difference.

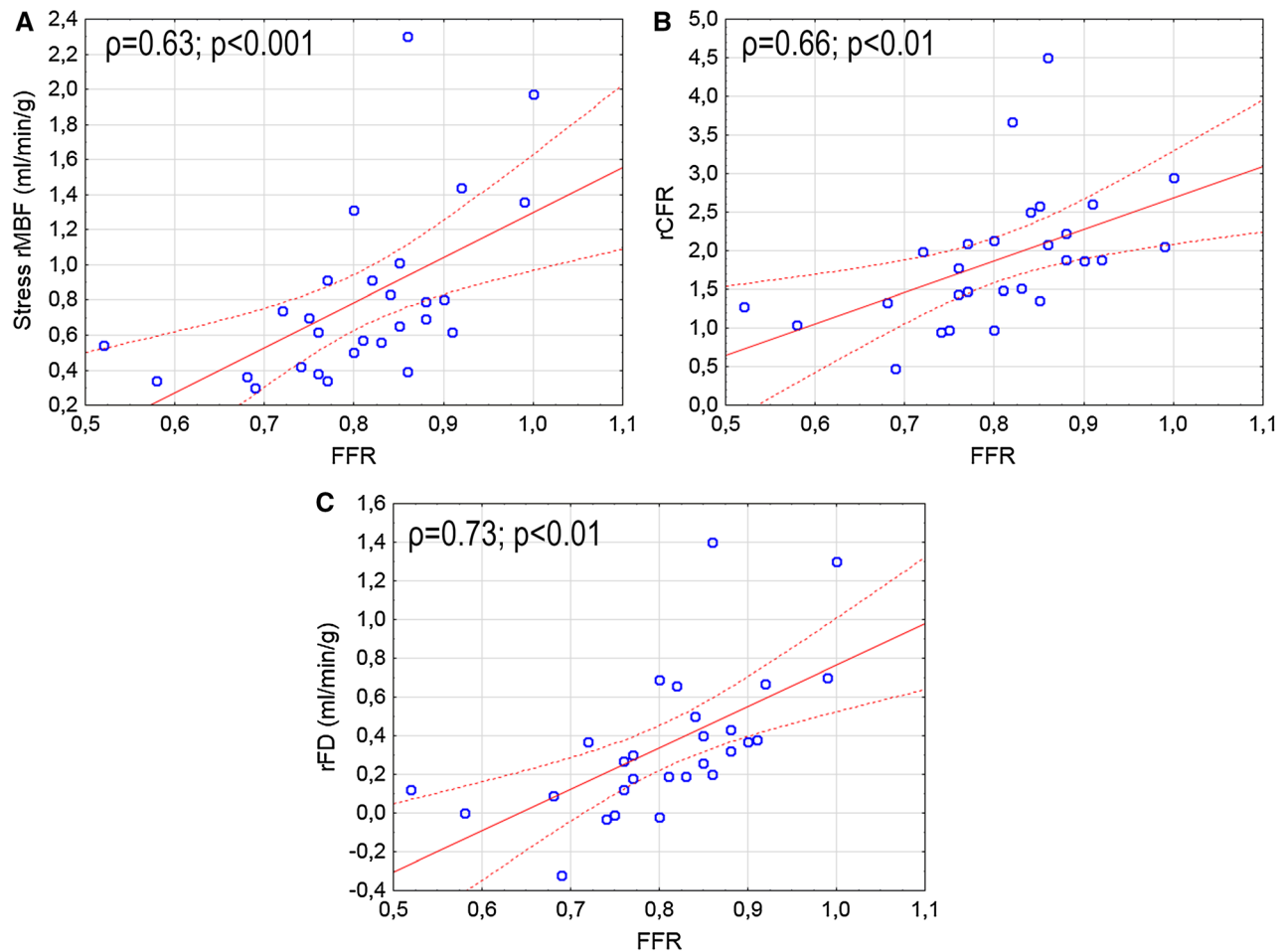


**Figure 2.** Correlations between FFR values and regional absolute myocardial perfusion parameters on CZT: (A) stress rMBF; (B) rCFR; (C) rFD. The solid line corresponds to the best-fit line and the dashed lines indicate the 95% mean confidence interval. *FFR*, fractional flow reserve; *stress rMBF*, regional myocardial blood flow; *rCFR*, regional coronary flow reserve; *rFD*, regional flow difference.

### Validation of Absolute MBF Analysis on Dynamic CZT vs FFR

In the last years, FFR has become gradually the ultimate gold standard for the definition of the functional severity of a given coronary luminal narrowing, by measuring the drop of distal intra-coronary pressure under conditions of pharmacologically induced maximal vasodilation.<sup>19,34–36</sup> Nevertheless, in the clinical setting consistent disagreement may still exist between FFR values and absolute MBF and CFR, as determined by PET imaging, possibly due to the variable effects of diffuse coronary atherosclerosis and/or microvascular dysfunction on coronary hemodynamics.<sup>37,38</sup> The disagreement with FFR evaluation becomes even greater when traditional cardiac imaging modalities is considered, with conventional SPECT imaging showing, at

best, a moderate accuracy in predicting the outputs of invasive assessment.<sup>39</sup> In this context, the introduction of dedicated cardiac cameras equipped with CZT detectors has allowed to increase significantly the accuracy of SPECT imaging, particularly in “risky” populations of patients, such as those with multiple vessel disease or non-obstructive CAD. Some previous groups have reported a comparison of CZT-derived MBF-estimates and either PET<sup>40</sup> or invasive coronary angiography plus FFR.<sup>41</sup> However, at variance with Wells et al<sup>40</sup> our study enrolled one half of patients with suspected CAD, resulting in an overall prevalence of significant coronary stenosis of 70%, a proportion that is more in line with the characteristics of the general patients population referred to myocardial stress imaging. On the other hand, at variance with Miyagawa et al<sup>41</sup> we used dynamic CZT acquisition not to derive a

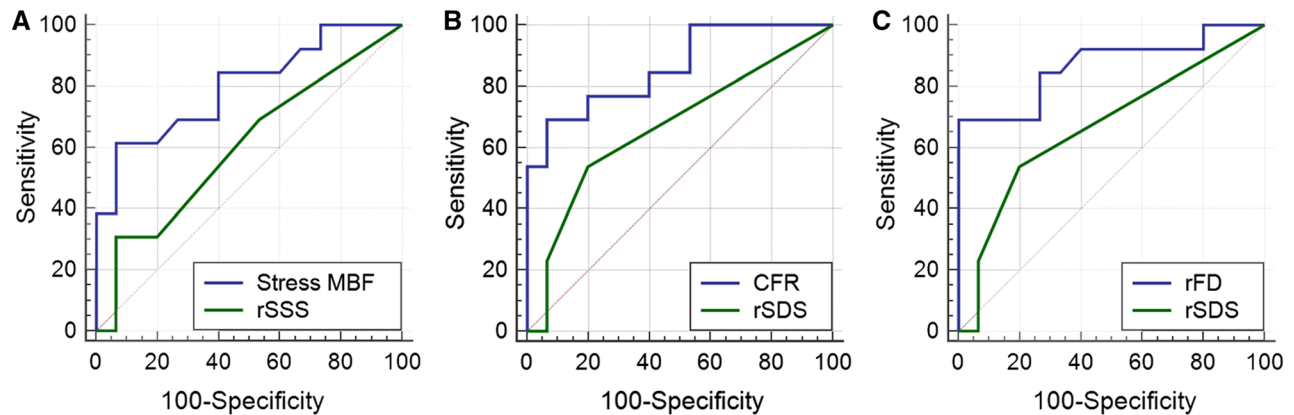


**Figure 3.** Area under receiver operating characteristic curves for regional semiquantitative MPI parameters and dynamic CZT derived myocardial blood flow indexes to predict ischemia by invasive FFR. (A) rSSS vs stress rMBF (0.6 mL/min/g and 0.8 mL/min/g; respectively,  $P = .1$ ). (B) rSDS vs rCFR (0.66 and 0.86;  $P = .06$ ). (C) rSDS vs rFD (0.66 mL/min/g and 0.89 mL/min/g, respectively;  $P = .03$ ). FFR, fractional flow reserve; stress rMBF, regional myocardial blood flow; rCFR, regional coronary flow reserve; rFD, regional flow difference; rSSS, regional summed stress score; rSDS, regional summed difference score.

mere estimate of myocardial perfusion (i.e. MFR index) but rather quantitative MBF and CFR, as the only physiologically meaningful parameters for the evaluation of patients with suspected significant CAD.

Moreover, disagreement exists on the most accurate methodology that should be applied to dynamic CZT analysis, particularly regarding attenuation correction and tracer's kinetic models. In this respect, we suppose, in line with previous similar papers<sup>40</sup> that attenuation correction is generally required when regional MBF analysis is performed. In fact, attenuation correction, by reducing the regional myocardial heterogeneity of CZT perfusion data, has been shown to increase the accuracy of MBF estimates when compared to PET. Accordingly, present results demonstrated the elevated accuracy of CZT-derived CFR in predicting pathologic FFR values, with a higher sensitivity than traditional semiquantitative perfusion variables. Furthermore, while a certain underestimation of hyperemic MBF data can be expected if compared with PET, the values of MBF and CFR that were obtained in our study compare well with the ones previously demonstrated using the same methodology in a similar patients population, demonstrating the strength of the technique.<sup>7</sup> Nevertheless, further evaluation in a more numerous population of patients will be needed to demonstrate clearly the additive clinical impact of MBF quantitation on dynamic CZT imaging.

## Limitations

The power of this study is limited by the small number of enrolled patients and that the FFR analysis was utilized only in a minority of stenoses. However, the consecutive nature of the enrollment coupled with the absence of almost any relevant exclusion criteria assures the selection of a cohort of subjects that represent a reliable picture of the ones in whom cardiac imaging is clinically indicated for the evaluation of suspected myocardial ischemia. The estimates of MBF and CFR obtained in our study differ from the ones recently reported with dynamic CZT imaging.<sup>6,42</sup> This difference could be explained by the dissimilar methodology of the two investigations, with the use of different kinetic models, and by the systematic use of attenuation correction of CZT images that was used in our study. In our study, most of the coronary stenoses were located in the LAD coronary artery. However, considering that attenuation correction of CZT data was systematically employed, there is no reason to believe that the distribution of CAD would have influenced the results of our analysis.

## NEW KNOWLEDGE GAINED

Information on the accuracy and clinical value of MBF and CFR quantification by CZT is still limited. In this study, the regional CZT-derived MBF, CFR and FD showed significant correlations with FFR values. Abnormal FFR values were best predicted by CZT-derived absolute stress MBF, CFR and FD compared with



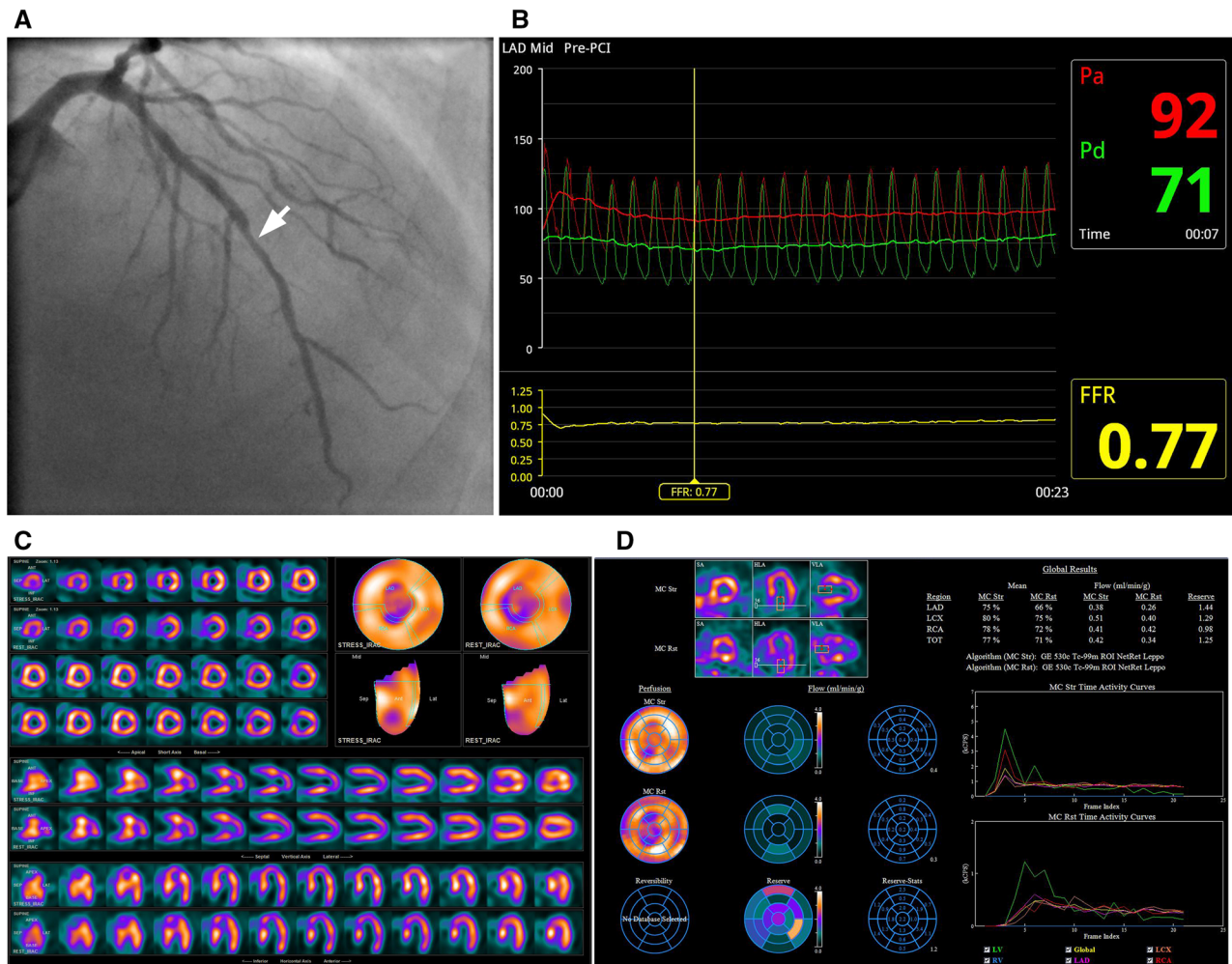


**Figure 4.** The example of a 67-year-old male, with right type of coronary supply, an intermediate (45%) but functionally significant (FFR 0.77) coronary lesion on the LAD coronary artery and no stenosis in LCX. The stenosis in mid segment of RCA was quantitatively considered as significant (> 75%) without FFR. Semiquantitative MPI underestimated LAD and RCA stenoses severity. (A) ICA of left coronary arteries showed intermediate stenosis (arrow) in the mid segment. (B) Phasic and mean aortic (red line) and distal (green line) coronary pressure during hyperemia. Fractional flow reserve in LAD is  $71/92 = 0.77$ . (C) SPECT MPI study at stress (top row) and rest (bottom row). (D) The results of dynamic CZT examination (LAD CFR 1.44; LCX CFR 1.29; RCA CFR 0.98).

standard MPI indexes (SSS, SDS). The study showed that absolute myocardial blood flow indexes predicting better the presence of ischemia (according FFR) than conventional semi-quantitative perfusion parameters.

### CONCLUSIONS

Our study shows that estimates of absolute myocardial perfusion parameters obtained through dynamic CZT acquisitions compare well with gold standard values computed with invasive FFR, predicting better

the presence of hemodynamically significant CAD than classical semi-quantitative perfusion parameters.

### Disclosure

Konstantin V. Zavadovsky, Andrew V. Mochula, Alla A. Boshchenko, Alexander V. Vrublevsky, Andrew E. Baev, Alexander L. Krylov, Marina O. Gulya, Evgeny A. Nesterov, Riccardo Liga and Alessia Gimelli declare that they have no conflict of interests.

## Ethical Approval

All procedures performed in studies involving human participants were in accordance with the ethical standards of the institutional and national research committee and with the 1964 Helsinki declaration and its later amendments or comparable ethical standards.

## Human and Animal Rights

This article does not contain any studies with animals performed by any of the authors.

## Informed Consent

Informed consent was obtained from all individual participants included in the study.

## Reference

- Murthy VL, Bateman TM, Beanlands RS, Berman DS, Borges-Neto S, Chareonthaitawee P, et al. Clinical quantification of myocardial blood flow using PET: Joint position paper of the SNMMI cardiovascular council and the ASNC. *J Nucl Cardiol* 2018;25:269-97.
- Ziadi MC. Myocardial flow reserve (MFR) with positron emission tomography (PET)/computed tomography (CT): clinical impact in diagnosis and prognosis. *Cardiovasc Diagn Ther* 2017;7:206-18.
- Kajander SA, Joutsiniemi E, Saraste M, Pietilä M, Ukkonen H, Saraste A, et al. Clinical value of absolute quantification of myocardial perfusion with (15)O-water in coronary artery disease. *Circ Cardiovasc Imaging* 2011;4:678-84.
- Wells RG, Timmins R, Klein R, Lockwood J, Marvin B, deKemp RA, et al. Dynamic SPECT measurement of absolute myocardial blood flow in a porcine model. *J Nucl Med* 2014;55:1685-91.
- Ben-Haim S, Murthy VL, Breault C, Allie R, Sitek A, Roth N, et al. Quantification of myocardial perfusion reserve using dynamic SPECT imaging in humans: A feasibility study. *J Nucl Med* 2013;54:873-9.
- Agostini D, Roule V, Nganoa C, Roth N, Baavour R, Parienti J-J, et al. First validation of myocardial flow reserve assessed by dynamic 99mTc-sestamibi CZT-SPECT camera: Head to head comparison with 15O-water PET and fractional flow reserve in patients with suspected coronary artery disease. The WATERDAY study. *Eur J Nucl Med Mol Imaging* 2018;45:1079-90.
- Nkoulou R, Fuchs TA, Pazhenkottal AP, Kuest SM, Ghadri JR, Stehli J, et al. Absolute myocardial blood flow and flow reserve assessed by gated SPECT with cadmium-zinc-telluride detectors using 99mTc-tetrofosmin: Head-to-head comparison with 13N-ammonia PET. *J Nucl Med* 2016;57:1887-92.
- Henzlova MJ, Duvall WL, Einstein AJ, Travin MI, Verberne HJ. ASNC imaging guidelines for SPECT nuclear cardiology procedures: Stress, protocols, and tracers. *J Nucl Cardiol* 2016;23:606-39.
- Neglia D, Rovai D, Caselli C, Pietila M, Teresinska A, Aguadé-Bruix S, et al. Detection of significant coronary artery disease by noninvasive anatomical and functional imaging. *Circ Cardiovasc Imaging* 2015;8:e002179.
- Cerqueira MD, Weissman NJ, Dilsizian V, Jacobs AK, Kaul S, Laskey WK, et al. Standardized myocardial segmentation and nomenclature for tomographic imaging of the heart. A statement for healthcare professionals from the Cardiac Imaging Committee of the Council on Clinical Cardiology of the American Heart Association. *Circulation* 2002;105:539-42.
- Leppo JA, Meerdink DJ. Comparison of the myocardial uptake of a technetium-labeled isonitrile analogue and thallium. *Circ Res* 1989;65:632-9.
- Yoshida K, Mullani N, Gould KL. Coronary flow and flow reserve by PET simplified for clinical applications using rubidium-82 or nitrogen-13-ammonia. *J Nucl Med* 1996;37:1701-12.
- Hutchins GD, Caraher JM, Raylman RR. A region of interest strategy for minimizing resolution distortions in quantitative myocardial PET studies. *J Nucl Med* 1992;33:1243-50.
- Renaud JM, DaSilva JN, Beanlands RSB, DeKemp RA. Characterizing the normal range of myocardial blood flow with <sup>82</sup>rubidium and <sup>13</sup>N-ammonia PET imaging. *J Nucl Cardiol* 2013;20:578-91.
- Tsuchida T, Yonekura Y, Takahashi N, Nakano A, Lee JD, Sadato N, et al. A trial for the quantification of regional myocardial blood flow with continuous infusion of Tc-99m MIBI and dynamic SPECT. *Ann Nucl Med* 1999;13:61-4.
- Camici PG, Rimoldi OE. The clinical value of myocardial blood flow measurement. *J Nucl Med* 2009;50:1076-87.
- DeLong ER, DeLong DM, Clarke-Pearson DL. Comparing the areas under two or more correlated receiver operating characteristic curves: A nonparametric approach. *Biometrics* 1988;44:837-45.
- Task Force Members, Montalescot G, Sechtem U, Achenbach S, Andreotti F, Arden C, et al. ESC guidelines on the management of stable coronary artery disease: The Task Force on the management of stable coronary artery disease of the European Society of Cardiology. *Eur Heart J* 2013;2013:2949-3003.
- Sousa-Uva M, Neumann F-J, Ahlsson A, Alfonso F, Banning AP, Benedetto U, et al. 2018 ESC/EACTS guidelines on myocardial revascularization. *Eur J Cardiothorac Surg* 2018;40:87.
- Danad I, Rajmakers PG, Driessen RS, Leipsic J, Raju R, Naoum C, et al. Comparison of coronary CT angiography, SPECT, PET, and hybrid imaging for diagnosis of ischemic heart disease determined by fractional flow reserve. *JAMA Cardiol* 2017;2:1100-7.
- Underwood SR, Anagnostopoulos C, Cerqueira M, Ell PJ, Flint EJ, Harbinson M, et al. Myocardial perfusion scintigraphy: The evidence. *Eur J Nucl Med Mol Imaging* 2004;31:261-91.
- Hida S, Chikamori T, Tanaka H, Igarashi Y, Shiba C, Hatano T, et al. Postischemic myocardial stunning is superior to transient ischemic dilation for detecting multivessel coronary artery disease. *Circ J* 2012;76:430-8.
- Beller GA. Underestimation of coronary artery disease with SPECT perfusion imaging. *J Nucl Cardiol* 2008;15:151-3.
- Berman DS, Kang X, Slomka PJ, Gerlach J, de Yang L, Hayes SW, et al. Underestimation of extent of ischemia by gated SPECT myocardial perfusion imaging in patients with left main coronary artery disease. *J Nucl Cardiol* 2007;14:521-8.
- Naya M, Murthy VL, Taqueti VR, Foster CR, Klein J, Garber M, et al. Preserved coronary flow reserve effectively excludes high-risk coronary artery disease on angiography. *J Nucl Med* 2014;55:248-55.
- van Werkhoven JM, Schuijff JD, Jukema JW, Kroft LJ, Stokkel MPM, Dibbets-Schneider P, et al. Anatomic correlates of a normal perfusion scan using 64-slice computed tomographic coronary angiography. *Am J Cardiol* 2008;101:40-5.
- Crea F, Camici PG, Bairey Merz CN. Coronary microvascular dysfunction: An update. *Eur Heart J* 2014;35:1101-11.
- Storto G, Cirillo P, Vicario MLE, Pellegrino T, Sorrentino AR, Petretta M, et al. Estimation of coronary flow reserve by Tc-99m sestamibi imaging in patients with coronary artery disease:

- comparison with the results of intracoronary Doppler technique. *J Nucl Cardiol* 2004;11:682-8.
29. Hsu B, Hu L-H, Yang B-H, Chen L-C, Chen Y-K, Ting C-H, et al. SPECT myocardial blood flow quantitation toward clinical use: a comparative study with (13)N-Ammonia PET myocardial blood flow quantitation. *Eur J Nucl Med Mol Imaging* 2017;44:117-28.
  30. Shrestha U, Sciammarella M, Alhassen F, Yeghiazarians Y, Ellin J, Verdin E, et al. Measurement of absolute myocardial blood flow in humans using dynamic cardiac SPECT and 99mTc-tetrofosmin: Method and validation. *J Nucl Cardiol* 2017;24:268-77.
  31. Shiraishi S, Sakamoto F, Tsuda N, Yoshida M, Tomiguchi S, Utsunomiya D, et al. Prediction of left main or 3-vessel disease using myocardial perfusion reserve on dynamic thallium-201 single-photon emission computed tomography with a semiconductor gamma camera. *Circ J* 2015;79:623-31.
  32. Ben Bouallègue F, Roubille F, Lattuca B, Cung TT, Macia J-C, Gervasoni R, et al. SPECT myocardial perfusion reserve in patients with multivessel coronary disease: Correlation with angiographic findings and invasive fractional flow reserve measurements. *J Nucl Med* 2015;56:1712-7.
  33. Lortie M, Beanlands RS, Yoshinaga K, Klein R, Dasilva JN, DeKemp RA. Quantification of myocardial blood flow with 82Rb dynamic PET imaging. *Eur J Nucl Med Mol Imaging* 2007;34(11):1765-74.
  34. Pijls NH, De Bruyne B, Peels K, Van Der Voort PH, Bonnier HJ, Bartunek J, Koolen JJ, et al. Measurement of fractional flow reserve to assess the functional severity of coronary-artery stenoses. *N Engl J Med* 1996;334:1703-8.
  35. Tonino PA, De Bruyne B, Pijls NH, Siebert U, Ikeno F, van't Veer M, et al. Fractional flow reserve vs angiography for guiding percutaneous coronary intervention. *N Engl J Med* 2009;360:213-24.
  36. Levine GN, Bates ER, Blankenship JC, Bailey SR, Bittl JA, Cercek B, et al 2011 ACCF/AHA/SCAI guideline for percutaneous coronary intervention: A report of the American College of Cardiology Foundation/American Heart Association Task Force on practice guidelines and the society for cardiovascular angiography and interventions. *Circulation* 2011;124:e574-651.
  37. Johnson NP, Kirkeeide RL, Gould KL. Is discordance of coronary flow reserve and fractional flow reserve due to methodology or clinically relevant coronary pathophysiology? *JACC Cardiovasc Imaging* 2012;5:193-202.
  38. Danad I, Uusitalo V, Kero T, Saraste A, Raijmakers PG, Lammermsma AA, et al. Quantitative assessment of myocardial perfusion in the detection of significant coronary artery disease: cutoff values and diagnostic accuracy of quantitative [(15)O]H<sub>2</sub>O PET imaging. *J Am Coll Cardiol* 2014;64:1464-75.
  39. Melikian N, De Bondt P, Tonino P, De Winter O, Wyffels E, Bartunek J, et al. Fractional flow reserve and myocardial perfusion imaging in patients with angiographic multivessel coronary artery disease. *JACC Cardiovasc Interv* 2010;3:307-14.
  40. Wells RG, Marvin B, Poirier M, Renaud J, deKemp RA, Ruddy TD. Optimization of SPECT measurement of myocardial blood flow with corrections for attenuation, motion, and blood binding compared with PET. *J Nucl Med* 2017;58:2013-9.
  41. Miyagawa M, Nishiyama Y, Uetani T, Ogimoto A, Ikeda S, Ishimura H, et al. Estimation of myocardial flow reserve utilizing an ultrafast cardiac SPECT: Comparison with coronary angiography, fractional flow reserve, and the SYNTAX score. *Int J Cardiol* 2017;244:347-53.
  42. Han S, Kim Y-H, Ahn J-M, Kang S-J, Oh JS, Shin E, et al. Feasibility of dynamic stress 201Tl/rest 99mTc-tetrofosmin single photon emission computed tomography for quantification of myocardial perfusion reserve in patients with stable coronary artery disease. *Eur J Nucl Med Mol Imaging* 2018;45:2173-80.

**Publisher's Note** Springer Nature remains neutral with regard to jurisdictional claims in published maps and institutional affiliations.